Bioorganic & Medicinal Chemistry Letters 20 (2010) 1109–1113

Contents lists available at ScienceDirect

Bioorganic & Medicinal Chemistry Letters

journal homepage: www.elsevier.com/locate/bmcl

Discovery of carmegliptin: A potent and long-acting dipeptidyl peptidase IV inhibitor for the treatment of type 2 diabetes

Patrizio Mattei *, Markus Boehringer, Patrick Di Giorgio, Holger Fischer, Michael Hennig, Joerg Huwyler †, Buelent Koçer, Bernd Kuhn, Bernd M. Loeffler ‡, Alexander MacDonald §, Robert Narquizian, Etienne Rauber, Elena Sebokova, Urs Sprecher

F. Hoffmann-La Roche Ltd, Pharma Research, CH-4070 Basel, Switzerland

ARTICLE INFO

Article history:
Received 21 October 2009
Revised 3 December 2009
Accepted 4 December 2009
Available online 6 December 2009

Keywords:
Dipeptidyl peptidase-IV
Glucagon-like peptide 1
Structure-based drug design

ABSTRACT

Design, synthesis, and SAR are described for a class of DPP-IV inhibitors based on aminobenzo[*a*]quinolizines with non-aromatic substituents in the S1 specificity pocket. One representative thereof, carmegliptin (**8p**), was chosen for clinical development. Its X-ray structure in complex with the enzyme and early efficacy data in animal models of type 2 diabetes are also presented.

Type 2 diabetes is a chronic, progressive metabolic disease, affecting about 4% of the world population. The main goal of the management of type 2 diabetes is to achieve glycemic control as close to the nondiabetic range as practicable, in order to reduce the risk of late-stage complications.[1] However, the therapeutic effect provided by existing medications is often not sustainable, since the multi-organ defects responsible for the disease are only insufficiently addressed.[2]

Dipeptidyl peptidase-IV (DPP-IV) inhibitors have emerged as a new therapeutic option to treat type 2 diabetes.[3–7] Their rapid rise in popularity is due to the favourable safety profile (no hypoglycemia, no weight gain, no gastrointestinal problems—typical side effects associated with established anti-diabetic agents). DPP-IV is a ubiquitous serine protease, the inhibition of which prevents the degradation of glucagon-like peptide 1 (GLP-1). The resulting higher levels of GLP-1 have a beneficial impact on major players involved in the pathogenesis of type 2 diabetes: β-cells, liver, α-cells, gut, and brain.[2] Long-term studies with DPP-IV inhibitors in patients are underway in order to confirm the safety and sustainability of these effects, and, in particular, their ability to prevent the progressive loss of β-cell function.

The preceding Letter describes the elaboration of (hetero-)aryl substituted aminobenzo[*a*]quinolizines, a class of highly potent DPP-IV inhibitors.[8] Here, we disclose the discovery of carmegliptin (**8p**), a DPP-IV inhibitor which has completed clinical phase 2 studies.

The co-crystal structure of butyl-amino[*a*]benzoquinolizine HTS hit **1** (IC_{50} = 520 nM) with DPP-IV (Fig. 1) reveals a favourable π–π stacking of the aromatic portion of the ligand with Phe357 and three symmetric H-bonds of the positively charged amino group with Glu205, Glu206, and Tyr662 as important interaction motifs. The *n*-butyl substituent points into the hydrophobic S1 specificity pocket further enhancing binding affinity. From overlay of this X-ray structure with that of the substrate analogue Val-pyrrolidide (**2**),[9] two shortcomings of the HTS hit become immediately apparent (Fig. 1). First, the S1 pocket is big enough to accommodate cyclic substituents and is not optimally filled by the *n*-butyl substituent. Second, the amino group of Asn710 is not satisfied in H-bonding interactions suggesting a desolvation penalty in this region. In the DPP-IV/Val-pyrrolidide structure, the C=O group of the ligand induces a slight turn of the terminal amide group resulting in the formation of an H-bond with the NH_2 group. This 3D-structure-based hypothesis is supported by SAR data generated in other series, as reported previously.[8,10] Thus, we focused our optimisation strategy on replacement of the *n*-butyl group with cyclic systems containing acceptor motifs that can potentially interact with the amido group of Asn710 as well as with the positive charge of Arg125.

* Corresponding author. Tel.: +41 61 6885438.
E-mail address: patrizio.mattei@roche.com (P. Mattei).
† Present address: University of Applied Sciences Northwestern Switzerland, Institute of Pharmaceutical Technology, Gründenstrasse 40, CH-4132 Muttenz, Switzerland.
‡ Present address: IPAM® Institut für praeventive und aesthetische Medizin, Knesebeckstrasse 68/69, DE-10623 Berlin, Germany.
§ Present address: GlaxoSmithKline, Medicines Research Centre, Gunnels Wood Road, Stevenage SG1 2NY, UK.

0960-894X/$ - see front matter © 2009 Elsevier Ltd. All rights reserved.
doi:10.1016/j.bmcl.2009.12.024

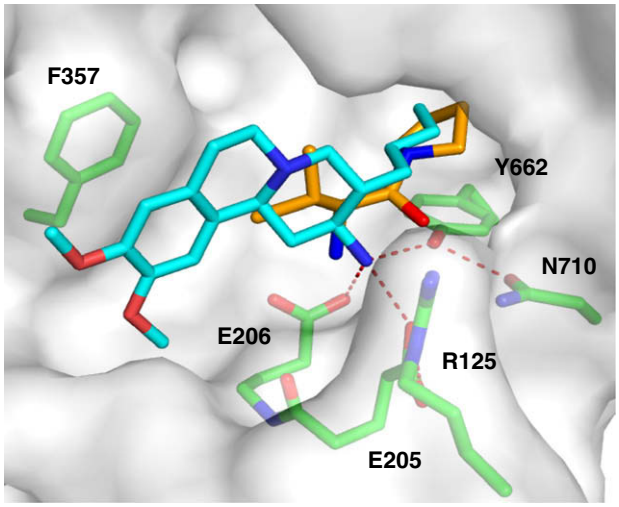

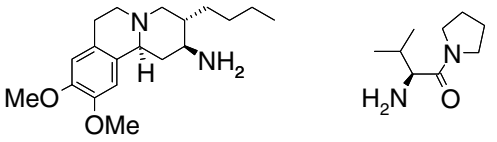

1 2

Figure 1. X-ray complex structure of DPP-IV (green) with aminobenzo[*a*]quinolizine HTS hit **1** (cyan; PDBid: 3kwh). Superimposed is the substrate analogue Val-pyrrolidide **2** (orange, PDBid: 1n1m). Hydrogen bonds are displayed in red.

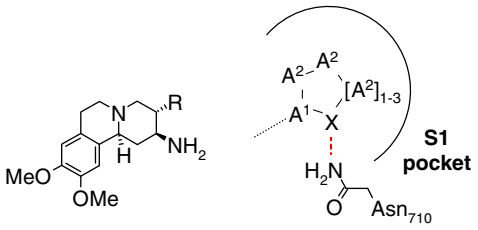

Scheme 1. Design of polar substituents to fill the S1 pocket of DPP-IV. X represents an H-bond acceptor functionality, such as C=O.

Our design strategy is depicted in Scheme 1.[11] An initial selection of ring systems of sizes 5–7 was obtained from virtual screening of monocyclic (hetero-)aromatic and -aliphatic rings from external and proprietary reagent databases, and subsequent modelling of their structural fit in the binding site. From this, N-substituted lactams [A^1 = N, A^2 = CH_2, X = C(=O)] of different ring sizes emerged as particularly interesting S1 substituents.

The synthesis of the target compounds is outlined in Scheme 2.[12] Thus, β-enol ester **3**[13] was converted to the corresponding β-enamino ester, followed by reduction with sodium borohydride/TFA[14] and protection of the primary amino group. This sequence gave the (*SR,SR,SR*)-stereoisomer **4** as the predominant product, which could be easily precipitated from the unwanted stereoisomers and impurities. The ester group was hydrolysed, and the resulting carboxylate salt was directly subjected to a Curtius rearrangement, using diphenyl phosphoryl azide.[15] Fluoride-mediated cleavage of the 2-(trimethylsilyl)ethyl carbamate group gave amine **5**. The heteroaliphatic head group was installed by acylation with acyl or sulfonyl chloride **6**, followed by cyclisation of **7** under basic conditions. Finally, acidic cleavage of the *tert*-butyl carbamate furnished compounds of formula **8**.

Compounds **8** were tested for inhibition of human DPP-IV. In a comparison of unsusbstituted lactams **8a–c**, the piperidinone **8b** is clearly the most potent one (Table 1). Neither pyrrolidinone **8a** (too small) nor azepanone **8c** can adequately occupy the S1 pocket.

The corresponding sultams **8d** and **8e** are less potent, presumably due to their higher steric demand and their less optimal alignment for H-bond interaction with Asn710. Similarly, the cyclic carbonates **8f** and **8g** are less potent than the corresponding lactams; here, a significant desolvation penalty of the carbamate oxygen upon binding to the hydrophobic cavity of the S1 pocket is likely.

The racemate **8b** was separated into its enantiomers using chiral HPLC (Chiralpak® AD). Only the (*S,S,S*)-enantiomer **8ba** is active. In comparison with the HTS hit **1** and the previous class of (hetero-)aryl-aminobenzo[*a*]quinolizines,[8] **8ba** is more hydrophilic and less amphiphilic. As a consequence, **8ba** does not induce phospholipidosis in vitro at any of the concentrations tested (test range: 2.5–20 μM).[16,17] Moreover, it is devoid of any significant hERG channel inhibition (patch-clamp assay;[18] highest concentration tested: 30 μM—for comparison, HTS hit **1** inhibits hERG channel by 45% at 10 μM). The compound is inert against metabolism, both in vitro (microsomes, hepatocytes) and in vivo, however, medium clearance is observed in vivo due to a likely combination of renal and biliary clearance of the parent. In rats, **8ba** is reasonably well absorbed and exhibits a high volume of distribution, and a half life of 4.5 h (Table 2). In an oral glucose tolerance test performed in insulin-resistant Zucker fatty (*fa/fa*) rats, **8ba** at a dose of 0.3 mg kg^{-1} reduces by 56% the glucose excursion 40 min after the glucose challenge.

The attractive profile of **8ba** encouraged us to further optimise the S1 pocket substituent within the lactam class. In the preceding paper, which describes the optimisation of (hetero)aryl S1 substituents, we obtained large affinity gains by introducing small substituents in the *meta*-position.[8] In comparison with piperidinone **8b**, the potency is slightly improved by methylation at C(4) (**8h**)

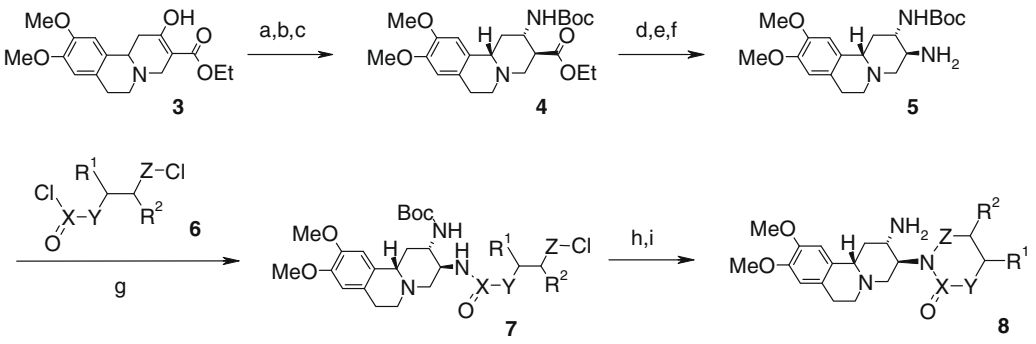

Scheme 2. Reagents and conditions: (a) NH_4OAc, MeOH, rt, 95%; (b) $NaBH_4$, TFA, THF, 0 °C; (c) Boc_2O, CH_2Cl_2, 83% over 2 steps; (d) KOH, aq THF, rt; (e) DPPA, Et_3N, 2-(trimethylsilyl)ethanol, toluene, 80 °C; (f) Et_4NF, CH_3CN, 50 °C, 56% over 3 steps; (g) Et_3N, CH_2Cl_2, (h) NaH, cat. NaI, DMF; (i) HCl, 1,4-dioxane.

Table 1
Structure–activity relationship of compounds **8**

Cpd	Stereochemistry[a]	X	Y	Z	R^1	R^2	IC_{50}[b] (nM)	log $D_{7.4}$[c]	P_e[d]	$\Delta\Delta G_{am}$[e]	In vitro PL[f]	$\Delta_{Glucose}$ (40′)[g]
8a	(*SR,SR,SR*)	C	CH_2	—	H	H	510	−0.5	0.6	−5.18	n.t.	n.t.
8b	(*SR,SR,SR*)	C	CH_2	CH_2	H	H	30	−0.5	0.2	−5.39	n.t.	−33%
8ba	(*S,S,S*)	C	CH_2	CH_2	H	H	22	−0.5	0.2	−5.39	>20	−56%
8bb	(*R,R,R*)	C	CH_2	CH_2	H	H	7800	n.t.	n.t.	−5.39	n.t.	n.t.
8c	(*SR,SR,SR*)	C	CH_2	CH_2CH_2	H	H	430	n.t.	n.t.	−5.86	n.t.	n.t.
8d	(*SR,SR,SR*)	S(O)	CH_2	—	H	H	1330	−0.7	1.2	−5.23	n.t.	n.t.
8e	(*SR,SR,SR*)	S(O)	CH_2	CH_2	H	H	142	−0.4	0.7	−5.35	n.t.	−18%
8f	(*SR,SR,SR*)	C	O	—	H	H	1150	−0.8	0.0	−5.58	n.t.	n.t.
8g	(*SR,SR,SR*)	C	O	CH_2	H	H	142	−0.9	0.10	−5.40	n.t.	n.t.
8h	(*SR,SR,SR*)	C	CH_2	CH_2	CH_3	H	19	−0.2	0.5	−5.84	n.t.	−16%
8i	(*SR,SR,SR*)	C	CH_2	CH_2	H	CH_3	3.7	0.0	1.1	−5.96	>20	−34%
8j	(*SR,SR,SR*)	C	CH_2	—	CH_3	H	9.3	−0.2	0.2	−5.56	>20	−42%
8k	(*SR,SR,SR*)	C	CH_2	—	CH_2CH_3	H	13	−0.1	0.9	−6.10	n.t.	−31%
8l	(*SR,SR,SR*)	C	$CH(CH_3)$	—	H	H	10,000	n.t.	n.t.	−5.47	n.t.	n.t.
8m	(*SR,SR,SR*)	C	CH_2	—	H	CH_3	2200	n.t.	n.t.	−5.46	n.t.	n.t.
8n	(*S,S,S*)	C	CH_2	—	(*S*)-CH_3	H	13	−0.1	0.6	−5.56	>20	−79%
8o	(*S,S,S*)	C	CH_2	—	(*R*)-CH_3	H	2.6	−0.3	0.8	−5.56	n.t.	−46%
8p	(*S,S,S*)	C	CH_2	—	(*S*)-CH_2F	H	6.8	−0.5	0.13	−5.43	>20	−66%
8q	(*S,S,S*)	C	CH_2	—	(*R*)-CH_2F	H	3.6	−0.4	0.4	−5.43	>20	−77%

[a] Tricyclic benzo[*a*]quinolizine subunit.
[b] For a description of experimental details see: Ref. 27.
[c] Permeability coefficient at pH 6.5 [10^{-6} cm^{-1}], determined by the parallel artificial membrane permeability assay (PAMPA).[28]
[d] Distribution coefficient at pH 7.4.[29]
[e] Calculated free energy of amphiphilicity, [kJ mol^{-1}].[30]
[f] Lowest concentration [μM] to induce phospholipidosis in vitro.[16]
[g] Reduction of glucose levels in *fa/fa* rats (oral glucose tolerance test), 40 min after glucose challenge (2 g kg^{-1}) compared to non treated animals; 0.3 mg kg^{-1} of DPP-IV inhibitor given 2 h before glucose challenge.

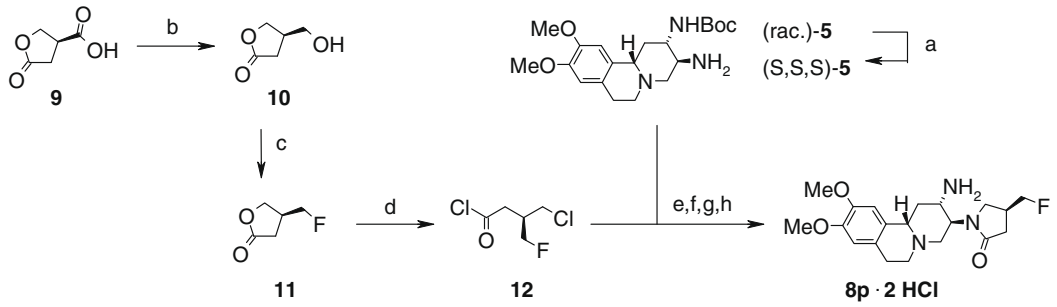

Scheme 3. Reagents and conditions: (a) preparative HPLC (Chiralpak® AD column), heptane/2-propanol 85:15, 37% (b) $BH_3{\cdot}Me_2S$, THF, 0 °C; (c) $(MeOCH_2CH_2)_2NSF_3$, CH_2Cl_2, 67% (2 steps); (d), $SOCl_2$, $ZnCl_2$, 80 °C, 72 h, 61%; (e) Et_3N, CH_2Cl_2; (f) NaH, DMF, 56% (2 steps); (g) HCl, 1,4-dioxane, 91%; (h) HCl, 2-propanol, 86%.

and, more significantly, at C(5) (**8i**). However, pyrrolidinone **8a** offers substantially more room for gaining affinity by alkylation at the correct position. Thus, 4-methylpyrrolidinone **8j** has an IC_{50} of 9.3 nM (about a 50-fold improvement over **8a**), and only minimal hERG inhibition (9% at 10 μM). 4-Ethylpyrrolidinone **8k** is equally potent but also more amphiphilic and inhibits hERG to an appreciable degree (45% at 10 μM). In accordance with expectation based on the rigidity of the S1 pocket, the regioisomeric methylpyrrolidinones **8l** and **8m** are only weakly active, underscoring the importance of achieving both the correct steric and electronic nature of the ligand within the cavity.

The individual isomers of the most promising compound, the 4-methylpyrrolidinone **8j**, were prepared in enantiomerically pure form (**8n**, **8o**). Since subtle changes in the S1 pocket can have a significant impact,[8] the 4-fluoromethyl-pyrrolidinones, **8p** and **8q** were also made. The synthesis of **8p** is outlined in Scheme 3 and required the enantiopure building blocks (*S,S,S*)-**5** and **12**. (*S,S,S*)-**5** was obtained from the racemate by preparative chiral HPLC. Acid chloride **12** was prepared starting from (*S*)-paraconic acid (**9**).[19] Reduction of **9** with borane–dimethyl sulfide complex afforded hydroxymethyl lactone **10**. Since **10** is known to racemise rather readily,[20] it was immediately treated with bis(2-methoxyethyl)aminosulfur trifluoride,[21] thereby affording fluoromethyl lactone **11**. This was converted to **12** by reaction with thionyl chloride in the presence of zinc chloride. The endgame of the synthesis proceeded uneventfully, in analogy with Scheme 2. The (*S*)-4-fluo-

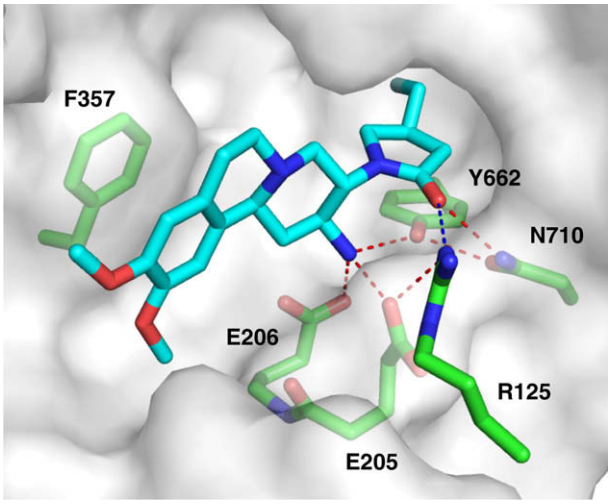

Figure 2. Crystal structure of DPP-IV with **8p**. Hydrogen bonds are shown in red and cation–dipole interactions in blue.

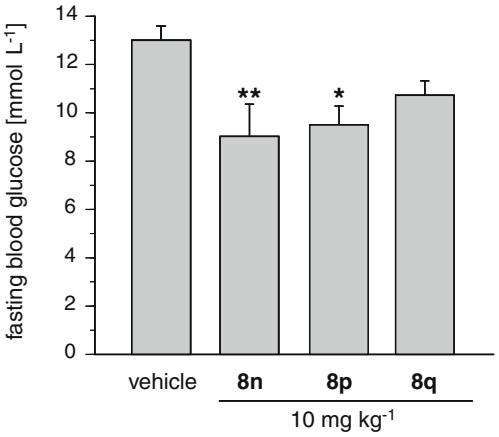

Figure 3. Levels of fasting blood glucose in db/db mice ($n = 6$/group; age 14 weeks), 2 h after compound administration per os. $^{*}p \leqslant 0.05$ or $^{**}p \leqslant 0.01$ compared to vehicle; ANOVA followed by Dunnett's post-hoc test.

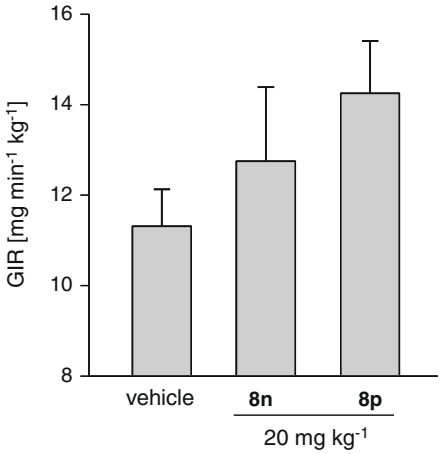

Figure 4. Glucose infusion rate (GIR) after administration of DPP-IV inhibitors **8n** and **8p** (20 mg kg^{-1} per day) for 7 days to Zucker fatty (*fa/fa*) rats in a euglycemic hyperinsulinemic clamp.

romethyl-pyrrolidinone **8p** was isolated as the dihydrochloride salt, a highly water soluble white crystalline solid, mp >275 °C.

In vitro, the substituted pyrrolidinone derivatives **8n–q** are all potent inhibitors of human DPP-IV (Table 1). To verify the modelled binding mode of this class, the crystal structure of **8p** with DPP-IV was determined at a resolution of 2.4 Å (Fig. 2).[22] The structure shows that the 4-fluoromethyl substituent occupies the lipophilic niche of the S1 pocket, in accordance with the significant affinity gain. The lactam C=O dipole makes favourable contacts with the amido NH_2 of Asn710 through a hydrogen bond ($d = 2.7$ Å) and with the guanidine tail of Arg125 through a cation-dipole interaction ($d = 3.0$ Å). It successfully mimics the amide carbonyl found in substrates and substrate analogues (P2 amide recognition site). Apart from the two additional pairwise interactions, the lactam C=O completes a cyclic network of favourable polar contacts involving Asn710, Tyr662, the primary amino group of **8p**, Glu205, and Arg125. In such an arrangement, cooperativity effects are likely.

Neither the stereochemistry of the substituent at C(4) nor the additional fluorine has a major influence on the IC_{50} (Table 1). However, **8p** and **8q** emerged as the most potent compounds when assessed by oral glucose tolerance tests in Zucker fatty (*fa/fa*) rats, on par with **8n**. These three compounds were also evaluated in hyperglycemic db/db mice. The data obtained in this model confirmed the improvement of glucose tolerance (the ΔAUC vs vehicle was −50%, - 30% and −20% for **8n**, **8p** and **8q**, respectively, during an oral glucose tolerance test using a dose of 10 mg kg^{-1}), but in addition a significant reduction of fasting blood glucose was demonstrated for **8n** and **8p** 2 h after compound administration (Fig. 3).

Furthermore, a sub-chronic efficacy study using a euglycemic hyperinsulinemic clamp[23] in Zucker fatty (*fa/fa*) rats (20 mg kg^{-1} over 7 days) was performed. In this experiment, both **8n** and **8p** improved insulin sensitivity, shown by the increased glucose infusion rate (GIR), but compound **8p** demonstrated slightly higher efficacy on GIR (Fig. 4) and also a trend for reduction of hepatic glucose production (−1.3 mg min^{-1} kg^{-1} vs vehicle).

Compound **8p** is selective for DPP-IV. Standard selectivity screenings[24] (ExpresSProfile—50 targets; non-kinase enzyme profile—26 targets) revealed no significant (>30% at 10 μM) off-target activity. The selectivity over related proline-specific dipeptidyl peptidases[25,26] is >100-fold for DPP-8 and DPP-9 and >2000-fold for FAP and DPP-II. Compound **8p** is neither an inhibitor nor an inducer of CYP450 enzymes and is only a weak inhibitor of the hERG channel ($IC_{20} = 21$ μM).

The pharmacokinetic parameters of **8p** are in line with other representatives of the class (Table 2). Following a single oral dose of 3 mg kg^{-1} of **8p** in cynomolgus monkeys, plasma DPP-IV activity is inhibited in a sustained manner (ca. 40% and 60% remaining activity relative to baseline after 24 h and 48 h, respectively), in agreement with the plasma concentrations (Fig. 5). Compound **8p** is excreted unchanged into urine following administration to rats, dogs, and monkeys. The renal clearance is approximately 30% of

Table 2
Pharmacokinetic parameters of selected compounds

Compd	Species	Cl[a,b]	Rat V_{ss}[a,c]	$t_{½}$[a,d]	F[e]
8ba	Wistar rat	25	5.9	4.5	47
8ba	Monkey[f]	18.7	8.6	9.4	64
8p	Wistar rat	24	6.3	5.3	28
8p	Monkey[f]	8.5	3.3	6.8	33

[a] Dose: 1 mg kg^{-1} i.v.
[b] Clearance [mL min^{-1} kg^{-1}].
[c] Volume of distribution at steady state, [L kg^{-1}].
[d] Half life [h].
[e] Oral bioavailability [%] at 3 mg kg^{-1}.
[f] Cynomolgus monkey.

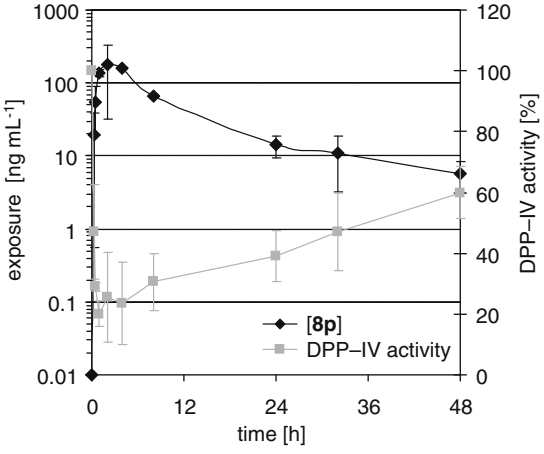

Figure 5. Plasma concentrations and relative plasma DPP-IV activity in cynomolgus monkeys after oral administration of **8p** (3 mg kg^{-1}). Values are the arithmetic means and standard deviations ($n = 2$).

total clearance in all species tested. Biliary excretion and intestinal secretion account for the rest of the clearance in the rat. This dual excretion mode has not been reported for any of the advanced DPP-IV inhibitors and may represent an advantage for patients with renal impairment. Taking together all pharmacological, DMPK and safety data, **8p** was selected for clinical development.

In summary, an X-ray guided design approach has led to the discovery of **8p** (INN: carmegliptin), a DPP-IV inhibitor with a tricyclic scaffold and a structurally distinct S1 recognition motif. Introduction of distributed patterns of polarity considerably contributed to the drug-likeness of the molecule. Carmegliptin exhibits a unique pharmacokinetic profile, with no metabolism and balanced renal and hepatic excretion. Clinical phase 1 and 2 studies have indicated its suitability as a safe oral anti-diabetic agent with once-daily administration. The results from these studies as well as the scalable synthesis and in-depth preclinical characterisation of carmegliptin will be reported in due course.

Acknowledgements

The authors gratefully acknowledge Vera Griesser, Marion Kaltenbacher, Angelina Wallier and Dr. Sabine Sewing for in vitro biological testing, Hans Gloor, Robert Wolfgang and Dr. Agnès Bénardeau for in vivo experiments, Dr. Ralf Thoma and Dr. Hans-Joachim Schönfeld for overexpression and purification of dipeptidyl peptidase enzymes, Dr. Liudmila Polonchuk for hERG measurements, Dr. Miklos Csato for in vitro phospholipidosis measurements, and Dr. Roger Norcross for careful proof-reading of the manuscript.

References and notes

1. Nathan, D. M.; Buse, J. B.; Davidson, M. B.; Ferrannini, E.; Holman, R. R.; Sherwin, R.; Zinman, B. *Diabetes Care* **2009**, *32*, 193.
2. DeFronzo, R. A. *Diabetes* **2009**, *58*, 773.
3. Villhauer, E. B.; Coppola, G. M.; Hughes, T. E. *Annu. Rep. Med. Chem.* **2001**, *36*, 191.
4. Drucker, D. J.; Nauck, M. A. *Lancet* **2006**, *368*, 1696.
5. Ahrén, B. *Expert Opin. Emerg. Drugs* **2008**, *13*, 593.
6. Pei, Z. *Curr. Opin. Drug Discov. Devel.* **2008**, *11*, 512.
7. Gwaltney, S. L., II *Curr. Top. Med. Chem.* **2008**, *8*, 1545.
8. Boehringer, M.; et al. Bioorg. Med. Chem. Lett. 2009. doi:10.1016/j.bmcl.2009.12.025.
9. Rasmussen, H. B.; Branner, S.; Wiberg, F. C.; Wagtmann, N. *Nat. Struct. Biol.* **2003**, *10*, 19.
10. Peters, J.-U.; Weber, S.; Kritter, S.; Weiss, P.; Wallier, A.; Boehringer, M.; Hennig, M.; Kuhn, B.; Loeffler, B.-M. *Bioorg. Med. Chem. Lett.* **2004**, *14*, 1491.
11. Virtual screening was performed in the following way: (a) selection of 2273 potential building blocks with MW <200 from the Available Chemicals Directory (ACD) and the Roche compound depository; (b) enumeration of a virtual library of aminobenzo[*a*]quinolizines with MOE (http://www.chemcomp.com/); (c) FlexX/Screenscore (Version 1.13.5, http://www.biosolveit.de/FlexX/) docking into the binding site of DPP-IV (PDBid: 3kwh) using the ring scaffold of the HTS hit **1** as base fragment reference (option SELBAS=reference) and a slightly increased tolerance for protein–ligand overlap (option MAX_OVERLAP_VOL=3.5); (d) visual inspection, filtering, and refinement of top 150 hits in Moloc (Gerber, P. R.; Mueller, K. *J. Comput. Aided Mol. Des.* **1995**, *9*, 251).
12. Boehringer, M.; Kuhn, B.; Mattei, P.; Narquizian, R. US Pat. Appl. 2004/0259903, 2004.
13. Brossi, A.; Lindlar, H.; Walter, M.; Schnider, O. *Helv. Chim. Acta* **1958**, *41*, 119.
14. Gribble, G. W. *Chem. Soc. Rev.* **1998**, *27*, 395.
15. Ninomiya, K.; Shioiri, T.; Yamada, S. *Tetrahedron* **1974**, *30*, 2151.
16. Lüllmann-Rauch, R.; Pods, R.; von Witzendorff, B. *Toxicology* **1996**, *110*, 27.
17. Fischer, H.; Kansy, M.; Potthast, M.; Csato, M. *Rational Approaches to Drug Design,* Proceedings of the European Symposium on Quantitative Structure–Activity Relationships, 13th, Düsseldorf, Germany, Aug 27–Sept 1, 2000, p 286.
18. Hamill, O. P.; Marty, A.; Neher, E.; Sakmann, B.; Sigworth, F. J. *Pflügers Arch.* **1981**, *391*, 85.
19. Crawforth, J. M.; Fawcett, J.; Rawlings, B. J. *J. Chem. Soc., Perkin Trans. 1* **1998**, 1721.
20. Mori, K.; Yamane, K. *Tetrahedron* **1982**, *38*, 2919.
21. Lal, G. S.; Pez, G. P.; Pesaresi, R. J.; Prozonic, F. M.; Chen, H. *J. Org. Chem.* **1999**, *64*, 7048.
22. The coordinates of the X-ray complex structure of human DPP-IV with compound **8p** have been deposited at the Protein Data Bank, accession code 3kwf.
23. Pospisilik, J. A.; Stafford, S. G.; Demuth, H.-U.; McIntosh, C. H. S.; Pederson, R. A. *Diabetes* **2002**, *51*, 2677.
24. Selectivity screenings were performed at Cerep S. A., Celle l'Evescault, France.
25. Van der Veken, P.; Haemers, A.; Augustyns, K. *Curr. Top. Med. Chem.* **2007**, *7*, 621.
26. Kirby, M.; Yu, D. M. T.; O'Connor, S.; Gorrell, M. D. *Clin. Sci.* **2010**, *118*, 31.
27. Lübbers, T.; Böhringer, M.; Gobbi, L.; Hennig, M.; Hunziker, D.; Kuhn, B.; Löffler, B.; Mattei, P.; Narquizian, R.; Peters, J.-U.; Ruff, Y.; Wessel, H. P.; Wyss, P. *Bioorg. Med. Chem. Lett.* **2007**, *17*, 2966.
28. Kansy, M.; Senner, F.; Gubernator, K. *J. Med. Chem.* **1998**, *41*, 1007.
29. Bendels, S.; Kansy, M.; Wagner, B.; Huwyler, J. *Eur. J. Med. Chem.* **2008**, *43*, 1581.
30. Fischer, H.; Kansy, M.; Bur, D. *Chimia* **2000**, *54*, 640.